American Society of Agricultural and Biological Engineers

An ASABE Meeting Presentation

Paper Number: **072146**

Evapotranspiration Mapping Using METRIC™ for a Region with Highly Advective Conditions

Jose L. Chavez, Agricultural Engineer, jchavez@cprl.ars.usda.gov

Prasanna H. Gowda, Agricultural Engineer, pgowda@cprl.ars.usda.gov

Terry A. Howell, Research Leader and Agricultural Engineer tahowell@cprl.ars.usda.gov
USDA-ARS Conservation and Production Research Laboratory (CPRL), P.O. Drawer 10, Bushland, TX, 79012-0010,

Thomas H. Marek, Agricultural Engineer, t-marek@tamu.edu
Texas Agricultural Experiment Station

Leon L. New, Professor, l-new@tamu.edu
Texas Cooperative Extension Service,

Written for presentation at the
2007 ASABE Annual International Meeting
Sponsored by ASABE
Minneapolis Convention Center
Minneapolis, Minnesota
17 - 20 June 2007

Abstract. *Agriculture in the Texas High Plains accounts for approximately 92% of groundwater withdrawals. Because, groundwater levels are declining in the region, efficient agricultural water use is imperative for sustainability and regional economic viability. Accurate regional evapotranspiration (ET) maps would provide valuable information on crop water demand and usage. In this study, a regional ET map was produced for an 11-county area in the Texas High Plains, using METRIC™ [a/] (Mapping Evapotranspiration at High Resolution using Internalized Calibration), a remote sensing based ET algorithm, and meteorological data measured at four ET weather stations maintained by the Texas High Plains Evapotranspiration Network (TXHPET). For this purpose, a Landsat 5 Thematic Mapper image acquired on 27 June 2005 was used. Performance of the ET model was evaluated by comparing predicted daily ET with values derived from a soil water budget at four different commercial irrigated fields. Good agreement was found between the remote sensing based ET and soil water budget ET for low to moderate ET rates. Less agreement resulted for higher ET rates. Use of METRIC™ for advective conditions of the Texas High Plains is promising; however, further evaluation is needed using lysimeter or Scintillometer derived ET measurements for different agroclimatological conditions and/or a larger number of image scenes.*

Keywords. *Ogallala Aquifer Region; Texas Panhandle; Regional ET; semi-arid environment*

[a/] Mention of trade or manufacturer names in this article is made for information only and does not imply an endorsement, recommendation, or exclusion by the United States Department of Agriculture.

Introduction

The Ogallala Aquifer has been the main source of water supply for the High Plains population and is being depleted at an unsustainable rate (Axtell, 2006). Irrigation alone uses approximately 89% of the water pumped from the Ogallala aquifer, where the High Plains area represents 27% of the total irrigated land in the United States (Dennehy, 2000). For this reason and considering the trends in population growth, there is a tremendous emphasis for greater efficiency in irrigation water management for agriculture in the Texas High Plains.

Improvement in irrigation water management is achieved when beneficial crop water use is accurately quantified in time and space in order to provide a useful tool for decision making in terms of proper timing and amounts of water to apply. In this regard, remote sensing (RS) based evapotranspiration (ET) methods may have a fundamental role in the improvement of irrigation efficiency and management. Numerous RS algorithms have been developed in an effort to spatially estimate crop water consumption or ET and are being tested around the world. Most of these algorithms mainly solve the energy balance of the land surface for latent heat flux (LE) at the time of satellite or airborne RS system overpass, and use different techniques to extrapolate the instantaneous values to daily values (Chávez, 2005).

The Texas High Plains is a semi-arid region with a heterogeneous landscape in which irrigated fields are surrounded by dryland crops, fallow land, and/or rangeland. Therefore, advection of sensible heat flux from dry surfaces is a significant source of energy that has a major impact on ET from crop growing areas. For example, Tolk et al. (2006) reported an average ET rate of 11.3 mm d^{-1} for an irrigated alfalfa in Bushland, TX with ET for some days exceeding 15 mm d^{-1} due to regional advection. Trezza (2002) observed that the RS methodology based on the alfalfa reference ET fraction (ET_rF), for estimating daily ET for a variety of crops (potatoes, snap beans, wheat, sugar beets, etc.) at Kimberly, Idaho, worked better under advective conditions than the evaporative fraction (EF) suggested by Bastiaanssen et al. (1998) in the Surface Energy Balance Algorithm for Land (SEBAL). The energy balance method that uses ET_rF was further refined and incorporated in METRIC™ (Mapping ET at High Resolution using Internalized Calibration), a RS ET algorithm based on SEBAL, to estimate daily and seasonal ET. A full description of the METRIC™ can be found in Allen et al. (2005a)

The main objective of this study was to assess the ability and usefulness of METRIC™ for mapping regional ET on the Texas High Plains. METRIC™ was selected as an ET mapping tool to be applied and evaluated in the Texas High Plains since it could be an algorithm that performs better under advective conditions and requires minimal ground data.

Materials and Methods

Study Area

This study was focused on the portion of the Texas High Plains Region (Panhandle counties) covered by Landsat 5 Thematic Mapper (TM) scene with a path/row of 30/35. The TM scene comprised 11 counties, underlain by the diminishing Ogallala aquifer (Fig. 1). Soils are mainly Pullman clay loam and Sherm silty clay loam (NCSS Web Soil Survey, 2006). Land use/cover in the study area consists of crops (described later), mesquite shrubs (grassland), mesquite brush, sandsage (Harvard Shin oak brush), buffalo grass (grassland), cottonwood-hackberry-salt cedar brush/wood, and mesquite-juniper brushes (Frye et al., 2000). More detailed analysis was concentrated in Ochiltree County located at the center of the scene, where ground truth data were acquired as part of another study. The Ochiltree County area is

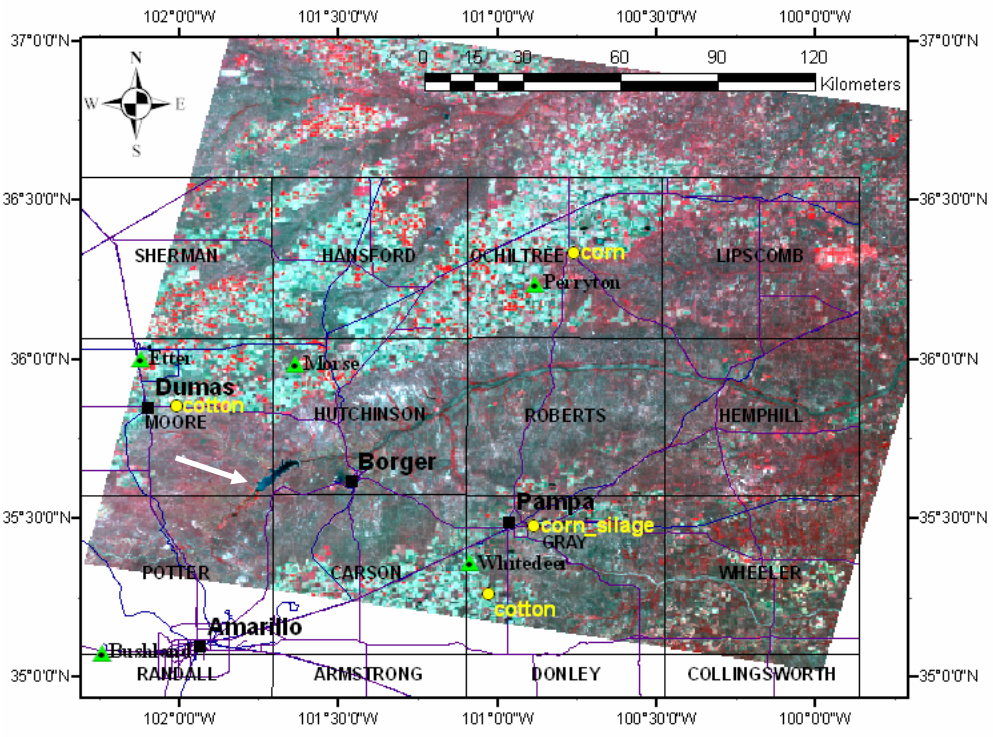

Figure 1. False color Landsat 5 TM image acquired on June 27 2005 covering several Counties of the Texas Panhandle.

about 234,911 ha with 44% of the land in row crop production. Annual average precipitation is approximately 562 mm, and about 11% of the cropland is irrigated with Ogallala Aquifer water. Sorghum, wheat and corn are the major crops in the county. Sherm silty clay soils with nearly level to gently sloping fields occupy most of the cropland. Wind direction is predominantly from the southwest direction.

Metric™

In METRIC™, ET is computed as a residual from the surface energy balance equation as an instantaneous ET or latent heat flux (LE) for the time of the satellite overpass, as in Eqn. (1).

$$LE = R_n - G - H \quad (1)$$

where R_n is net radiation (W m^{-2}), G is the soil heat flux (W m^{-2}), and H is the sensible heat flux (W m^{-2}). LE is converted to ET (mm h^{-1} or mm d^{-1}) by dividing it by the latent heat of vaporization (λ_{LE}; ~2.45 MJ kg^{-1}) and the density of water (ρ_w; ~1.0 Mg m^3). The sign convention for the different flux terms in Equation (1) is positive away from the surface (towards the atmosphere) for LE and H and positive towards the surface for R_n and G. R_n is calculated using surface reflectance and surface temperature (T_s) derived from the satellite imagery, near surface vapor pressure from a near-by weather station (WS), and R_s as explained below. R_n is the result of the surface energy budget between short and long wave radiation terms described as:

$$R_n = R_s\downarrow - \alpha R_s\downarrow + R_L\downarrow - R_L\uparrow - (1-\varepsilon_o)R_L\downarrow \quad (2)$$

where: $R_s\downarrow$ is incoming shortwave radiation (W m^{-2}), α is surface albedo (unitless), $R_L\downarrow$ is incoming long wave radiation (W m^{-2}) or downward thermal radiation flux originated from the atmosphere which can be estimated using the Stefan-Boltzmann equation and near surface air temperature as well as vapor pressure for air emissivity. In METRIC, $R_L\downarrow$ is estimated using T_s

and the broad band atmospheric transmissivity for short wave radiation. $R_L\uparrow$ is outgoing long wave radiation (W m^{-2}), and ε_o is broad-band surface thermal emissivity (unitless). The (1-ε_o)$R_L\downarrow$ term represents the fraction of incoming long wave radiation reflected from the surface. Surface albedo is the term that is a function of reflectance values in the shortwave portion of the electro-magnetic spectrum and $R_L\uparrow$ is the term that depends on T_s.

Soil heat flux (G) was modeled as a function of R_n, vegetation index, surface temperature, and surface albedo for near midday values according to the Bastiaanssen (2000) model. In METRIC^{TM}, H is estimated using a temperature difference (dT), function of T_s:

$$H = \rho_a Cp_a \frac{dT}{r_{ah}} \quad (3)$$

where: ρ_a is air density (kg m^{-3}), Cp_a is specific heat of dry air (1004 J kg^{-1} K^{-1}), r_{ah} is calculated between two near surface heights, z_1 and z_2 (generally 0.1 and 2 m) using a wind speed extrapolated from some blending height above the ground surface (typically 100 to 200 m) and an iterative stability correction scheme for atmospheric heat transfer based on the Monin-Obhukov stability length scale (L_MO, similarity theory; Foken, 2006). In this study, a height of 200 m was used in the calculation of distributed friction velocity (u*), a term utilized in the estimation of H. The expression [dT = *a* + *b* T_s] characterizes the relationship of dT to T_s where *a* and *b* are empirically determined constants.

Determination of coefficients *a* and *b* involves locating a hot (dry) pixel with a high T_s value and a cold (wet) pixel with a low T_s value (typically one in an irrigated agricultural setting) in the remote sensing image. Once these pixels have been identified, the energy balance of Equation (1) can be solved for H_{cold} and H_{hot} as $H_{cold} = (R_n - G)_{cold} - LE_{cold}$ and $H_{hot} = (R_n - G)_{hot} - LE_{hot}$. Where H_{hot} and H_{cold} are the sensible heat fluxes for the hot and cold pixels respectively. The hot pixel is defined as having no latent heat flux (i.e., all available energy is partitioned to H), although LE_{hot} may be calculated according to a soil water budget, for the hot pixel, if rainfall has occurred in the last couple of weeks before the image acquisition date. The cold pixel is assumed to have latent heat flux equal to 1.05 times that expected for a tall reference crop (i.e., alfalfa), thus LE_{cold} is set equal to 1.05 ET_r λ_{LE}, where ET_r is the hourly (or shorter time interval) tall reference (like alfalfa) ET calculated using the standardized ASCE Penman-Monteith equation. A 1.05 coefficient was used to estimate LE_{cold} as the cold pixels typically have an ET rate 5% larger than that for the reference ET (ET_r) due to wet soil surface beneath a full vegetation canopy that will tend to increase the total ET rate Allen et al. (2005b).

A hot pixel was chosen after careful screening of fallow/bare agricultural fields displaying high temperatures, high albedo and low biomass (leaf area index, LAI). Similarly, the cold pixel was determined on the basis of low temperature, high biomass, and albedo of approximately 0.18-0.24. With the calculation of H_{hot} and $H_{cold,}$ Equation 3 was inverted to compute dT_{hot} and dT_{cold}. The *a* and *b* coefficients were then determined by fitting a line through the two pairs of values for dT and T_s from the hot and cold pixels. These *a* and *b* values were initial values that were used in an iterative stability correction scheme programmed in an Excel^{TM} spreadsheet, which after some iterations shows numerical convergence and the *a* and *b* coefficient for each iteration were then exported to a model in ERDAS Imagine to obtain the final stability corrected H image.

Instantaneous LE image was obtained using Eqn. 1, and it was converted to ET_i in mm h^{-1} by dividing it by λ_{LE} and $\rho_w$as shown in Eqn. 4:

$$ET_i = 3600\ LE / \{[2.501 - 0.00236\ (T_s - 273.15)]\ (10^6)\ (1.0)\} \quad (4)$$

The reference ET fraction (ET_rF) is the ratio of ET_i to the reference ET_r that is computed from WS data at overpass time. The WS information is explained in a subsequent section. Finally, the computation of daily ET (ET_{24}), for each pixel, is performed as shown in Equation (5):

$$ET_{24} = ET_rF \times ET_r24 \quad (5)$$

where: ET_r24 is the cumulative 24-h ET_r for the day (mm d^{-1}).

Data

A Landsat 5 TM satellite image was obtained for DOY 178 (June 27) of 2005; the overpass time was 17:07 GMT. The satellite path/row was 30/35 where the image scene center coordinates were Latitude 36.048º N and Longitude 100.910º W. Image pixel size was 30 m for TM bands 1, 2, 3, 4, 5 and 7 and 120 m for TM band 6 (thermal band). However, the image supplier resampled TM band 6 to a 30 m pixel size. Figure 1 shows the satellite image in false color.

Ground truth data for Ochiltree County consisted of GPS readings taken in 29 fields to identify cover crops during the 2005 cropping season. This information was utilized in the un-supervised classification using the ERDAS Imagine 9.0 (Leica Geosystems Geospatial Imaging, LLC, Norcross, GA) to produce a land use map. The land use map was used to show the type of existing vegetation/crop cover as well as their spatial distribution, and ultimately to report actual water use (ET) by land use class.

For the calculation of alfalfa based ET_r and ET_r24, data from four reference WS (Perryton, Etter, White Deer, and Morse; Fig. 1) identified within the geographic coverage of the satellite scene were used. These WS are part of the Texas High Plains ET Network (TXHPET) and the Texas North Plains ET Network (TNPET). The TXHPET and TNPET reports hourly and daily weather data as well as grass (ET_o) and alfalfa (ET_r) reference ET calculated using the standardized ASCE Penman-Monteith method. The WS grass cover types were: native pasture (Perryton), Buffalo grass (Etter), native pasture (White Deer), and native grass (Morse). These grasses were rainfed with the exception of the Etter grass that was irrigated (limited).

Soil water content measurements from four commercial fields: 1) fully irrigated corn 2) irrigated silage corn, 3) irrigated cotton, and 4) on a cotton field under limited irrigation were used to derive ET for comparison with RS estimates. These measurements were taken as a part of the Agripartners Program (New, 2005). Soil water was monitored by means of a KS-D1 Gypsum block meter (Delmhorst Instruments Company, Towaco, NY) connected to GB-1 Gypsum blocks sensors. The blocks were installed at a depth of 0.3, 0.6, and 0.9 m, respectively, and readings were recorded twice each week. Although Gypsum block sensors are considered unreliable (Gardner, 1986), they perform well in fine texture soils (Yoder et al., 1998, Evans et al., 1996). In our case, most soils were clay loam and thus it is expected the sensors to perform better than reported in the literature. The date, number and amount of individual irrigations were recorded and calculated using deep well water flow deliveries (New, 2005). Rainfall data measured at the site were used.

Satellite image calibration involved conversion of digital number (DN) into radiance (L_b), for each band by means of calibration coefficients (L_b= (gain x DN) + bias). Then, to obtain “at-satellite” or at “Top-of-the-Atmosphere” (TOA) reflectance values, for the short-wave bands, the detected radiance at the satellite (for each band) was divided by the incoming energy (radiance) in the same short-wave band. In the case of the thermal band, the spectral radiance values were converted into effective at-satellite temperatures of the viewed Earth-atmosphere system under an assumption of unity surface emissivity and using pre-launch calibration constants by means of an inverted logarithmic formula. Detailed steps on the Landsat 5 TM radiometric calibration procedures can be found in Chander and Markham (2003). Subsequently, the at-surface

reflectance values were computed after applying atmospheric interference corrections, on the TOA reflectance image, for short- wave absorption and scattering using narrowband transmittance values for each band as calibrated by Tasumi et al. (2005).

METRIC^{TM} ET Evaluation

METRIC^{TM} ET estimates were compared with ET derived from soil water content readings (ET_c) at four different locations (Fig. 1) by means of the soil water balance (SWB):

$$ET_c = \theta_{i-1} - \theta_i + I + P \quad (6)$$

where: θ_i is the soil water (depth equivalent) in the root zone at the beginning of day "i", θ_{i-1} is the soil water equivalent in the root zone at the beginning of day "i-1", i.e. the previous day, I is net irrigation depth, and P is the rainfall. In this study, I was estimated from measured volumetric water deliveries, center pivot area and by assuming two water application efficiencies (E_a), 80 and 90%; these E_a values were published by New and Fipps (2000) for LESA center pivot irrigation systems as common for the Texas High Plains area. The SWB calculations were performed over a period of 3 or 4 days depending on the number of readings per week.

Results stemming from the comparison of ET using the METRIC^{TM} and the ET from soil water content measurements, for each field, were reported as absolute differences and in percent errors relative to ET_r as: Difference (%) = (ET_estimated – ET_observed) x 100 / ET_r. Where ET_estimated is the ET by METRIC^{TM} and ET_observed is ET derived from the soil water content balance. A more comprehensive evaluation of ET estimation errors (comparison of estimated/measured ET_c) was carried out comparing Mean Bias Error (MBE) and Root Mean Square Error (RMSE), expressed in percent. These are the mean and standard deviation errors respectively. Also, linear least squares regression method was utilized in evaluating estimated ET.

Results and Discussion

Cropping Conditions, Net radiation and heat fluxes

A land use map was derived from the Landsat 5 TM image. A subset of the land use map, comprising most of Ochiltree County, was analyzed. In this map, total area was 57,487.2 ha, of which most of the area was not irrigated, 58.4% of the area was either fallow fields/bare soils and/or natural vegetation (pasture, grass, shrubs, bushes) while the cropped land accounted for 39.5% of the area: 11.2% for irrigated corn (6,468 ha), 15% for irrigated soybean (8,664 ha), 8% for irrigated sorghum (4,615 ha), and 5.2% for both irrigated/non-irrigated cotton (3,004 ha). These results were matched well with corn and cotton crop acreage reported in the 2005 National Agricultural Statistics Report (USDA-NASS, 2006).

Surface temperatures derived from Landsat 5 TM scene ranged from 18.6 to 34.9°C. This variation highlights the uniqueness of cropping conditions in the Texas High Plains where irrigated/non-irrigated crop fields intermix with fallow/bare soil lands and where local and regional advection may increase ET rates by augmenting sensible heat flux. Tolk et al. (2006) found that an average of 61% of total ET could be attributed to advective sensible heat in Bushland, TX (Fig. 1), for average wind speeds of 4.4 m s^{-1}. In our study, wind speed (u) at the time of satellite overpass was 7.0 m s^{-1} (Perryton WS), i.e. higher than the values reported in Tolk et al (2006) and ranged between 7.5 and 8.5 m s^{-1} from noon to about 7:00 PM CST. In addition, more than half of the area was not irrigated and some irrigated cotton, soybean and sorghum fields were at very early growth stage (LAI<1.5) with partial canopy cover, a situation that may have contributed to local advective conditions for DOY 178.

Average R_n was 616.0 W m^{-2} for the entire scene with water bodies and recently irrigated fields having higher R_n values (690-750 W m^{-2}), non-water stress high biomass (LAI > 3.0) fields with similar R_n (600-650 W m^{-2}), and bare soils having lower R_n (500-550 W m^{-2}).

Average G value was 87 W m^{-2}: 370-380 W m^{-2} for Lake Meredith (water heat flux, WHF, Fig. 1), 80-100 W m^{-2} for bare soils, 50-60 W m^{-2} for shallow water bodies (playa lakes; WHF), and 25-40 W m^{-2} for high biomass crops.

In the determination of H, the colder (wet) pixel was located in a recently irrigated corn field that had surface temperature of 18.6ºC (291.7 K). It is about half a degree higher than the water temperature in Lake Meredith, thus the corn field was using available energy (AE = R_n-G) entirely in the ET process. The hotter (dry) pixel was found in a nearby fallow dry field. Table 1 reports ET_rF, T_s, R_n, G, roughness length for momentum transfer (Z_{om}), and wind speed at a blending height of 200 m for wet and dry pixels. Maximum wind speed at a height of 200 m was 14.4 m s^{-1}. For the hot pixel, ET_rF was assumed to be zero (0), i.e. no ET, since the last "significant" rainfall event occurred on June 12 (15 days prior to the satellite overpass) and the amount of daily rainfall varied from 7-44 mm in the study area.

Values in Table 1 were used in the initial estimation of dT and H, for both hot and cold pixels under neutral atmospheric conditions. Initial H and dT values were subsequently adjusted for the unstable atmospheric conditions encountered for DOY 178 using the Monin-Obukhov length scale iterative method. After four iterations, changes in r_{ah}, for the hot pixel, were below 0.5% thus meeting the convergence criteria of 5% difference in r_{ah} in each iteration cycle. Table 2 reports the resulting final values for r_{ah}, horizontal friction velocity (u_*), L_{MO}, dT, LE, and H for both cold and hot pixels.

Setting ET_rF to 1.05 for the cold pixel resulted in a negative H value, meaning that the air temperate was higher than the corn canopy temperature, thus extra heat was brought in by local and regional advection. This extra heat produced an H (cold pixel) that enhanced LE beyond available energy (633.9 W m^{-2}) by 24.4%. These results are in agreement with results reported by Tolk et al. (2006).

In Table 2, H for hot pixel was 425.6 W m^{-2} for a dT of 4.4 K (or ◦C). The (dT, H) pairs for both cold and hot pixels were used in the determination of the coefficients for Eqn. 3, which were *a* = 0.353 and *b* = -104.41. These coefficients, along with the intermediary coefficients found during

Table 1. Input data for H determination.

Variable	Units	Cold Pixel	Hot Pixel
Coordinates	X (UTM), m	320629.3	322235.2
Coordinates	Y (UTM), m	4005875.7	4006151.0
Elevation	m	907	907
ET_rF	unit less	1.05	0
T_s	K	291.7	308.0
R_n	W m^{-2}	695.0	532.0
G	W m^{-2}	61.1	106.4
Z_{om}	M	0.13	0.01
u(200 m)	m s^{-1}	14.4	14.4

Table 2. Atmospheric stability adjusted H

Variable	Unit	Cold Pixel	Hot Pixel
r_{ah}	s m^{-1}	9.5	10.7
u_*	m s^{-1}	0.78	0.62
L_{MO}	m	241.2	-44.2
dT	K	-1.36	4.43
LE	W m^{-2}	788.4	0
H	W m^{-2}	-154.5	425.6

the atmospheric stability correction process, were used in ERDAS Imagine modeler to get the H image.

Daily ET Estimation

Average daily ET (ET_{24}) was 5.7 mm d^{-1} with a mode and maximum values of 6.9 and 14.5 mm d^{-1}, respectively, for the entire satellite scene. Using all four WS in Table 3, the average ET_r was 13.5 mm d^{-1} for the day, and ET_r was 1.1 mm h^{-1} at the time of satellite overpass.

According to the ET_rF results in Table 3, the WS grasses had an ET rate that was only 43 to 51% of ET_r24 and 60 to 76% of the "potential" grass ET_o, i.e., to that rate of a non-water limited clipped grass; assuming that the calculated reference ET, with the weather parameters that incorporate advection, represent ET that otherwise would have been attained had the grass been fully irrigated (Howell, 2000).

Considering E_a of 90% for ET derivation through the SWB procedure, METRIC™ ET_{24} estimation for a fully irrigated corn compared reasonably with the crop ET (ET_c) derived from the soil water balance for the same corn field (Table 4). There was an overestimation error of 2.0 mm d^{-1} or a bias of 14.7% (relative to the four WS average ET_r). For the irrigated silage corn field, the error was 8.1%, 1.5% for irrigated cotton and –7.4% for the limited irrigated cotton field; with an average (overall) error of 1.1±0.9 mm d^{-1} or 8.0±6.5%, MBE±RMSE, respectively.

In the case of the soil water balance based ET_c, values obtained assuming an E_a of 80% resulted in ET_c average estimation errors of 2.1±1.3 mm d^{-1} or 15.2±9.5 %, MBE±RMSE respectively. Figure 2 shows the graphical comparison of estimated versus measured ET values for an E_a of 90 and 80%.

In general, the relative higher ET estimation error was found in the fully irrigated corn field, which had an ET rate closer to the reference crop ET rate. The higher discrepancy in ET may be due to the fact that the cold pixel(s) should be selected in a field with a crop with bio-physical characteristics similar to the alfalfa reference crop, i.e., similar biomass, height and fully-irrigated crop ET. However, errors could be introduced when the satellite image does not contain such crop conditions. Moreover, ET_{cold} is assumed by METRIC as 1.05 ET_r and it may happen that the selected cold pixel belongs to a crop with a crop coefficient (K_c) that is greater than 1.0 at the time of the image acquisition, which will increase its ET value beyond the 5% proposed for a crop with characteristics similar to the alfalfa reference crop hence resulting on an overestimation of ET for colder highly evapotranspirating pixels (crops). In our case, the cold pixel was located on a well irrigated corn field. Other crop fields had lower LAI values than most corn fields, had not reached full cover conditions, had higher T_s values and consequently were not candidates to be selected as cold pixels.

Table 3. Weather Stations reference ET and METRIC™ grass ET estimation.

Site	Weather Station		METRIC™			ET_o Difference	
	ET_o	ET_r	ET_{24}	ET_rF	ET_i	WS vs METRIC	
	mm d^{-1}	mm d^{-1}	mm d^{-1}		mm h^{-1}	mm d^{-1}	fraction
Perryton	9.9	14.4	5.9	0.43	0.47	-4.0	0.60
Etter	9.3	13.3	6.0	0.44	0.48	-3.3	0.65
White Deer	9.8	13.8	7.0	0.51	0.56	-2.8	0.71
Morse	9.2	12.9	7.0	0.51	0.56	-2.2	0.76

Note: ET_o has the same connotation as ET_{24} in this table.

Table 4. Corn and Cotton METRIC™ and soil water content balance based ET assuming an irrigation system application efficiency of 90%.

Crop	Soil water balance		METRIC™			ET_c Difference	
	ET_c (mm d^{-1})	K_c[1]	ET_{24} (mm d^{-1})	ET_rF	ET_i (mm h^{-1})	bias (mm d^{-1})	bias (%)
Fully irrigated corn	11.7	0.81	13.7	1.01	1.11	2.0	14.5
Irrigated silage corn	6.2	0.45	7.3	0.53	0.58	1.1	8.0
Limited irrigated cotton	1.4	0.10	0.4	0.03	0.03	-1.0	-7.2
Irrigated cotton	5.9	0.44	6.1	0.45	0.50	0.2	1.4
					MBE =	1.1	8.0
					RMSE =	0.9	6.5

Note: ET_c has the same connotation as ET_{24} in this table. [1]K_c – Based on WS ET_r

The underestimation error for ET_c of -7.4% for the cotton field that had limited irrigation may be due to that it was planted later in the season, had low biomass with partial canopy cover and surface temperatures were high (dT ~ 4 K).

METRIC™ captured the difference in water management between fully irrigated corn and somewhat water stressed silage corn as per the ET rates (Table 4), where the fully irrigated grain corn ET was almost double of that for silage corn. This result was supported by New (2005) where he showed that the amount of water applied to the grain corn as irrigation and rainfall was in excess of the corn potential ET (PET) as calculated by TXHPET.

Regional ET_{24} for the entire satellite scene are shown in Fig. 3, where darker dots are high ET rates mainly for center pivot irrigated corn and soybean fields. Irrigated corn had the greatest ET rate, 10.7±3.4 mm d^{-1}, i.e. from 7.3 to 14.1 mm d^{-1}. This result is in excellent agreement with a 3-yr study by Howell et al. (1996) and Howell et al. (1998) in Bushland-TX, where the authors

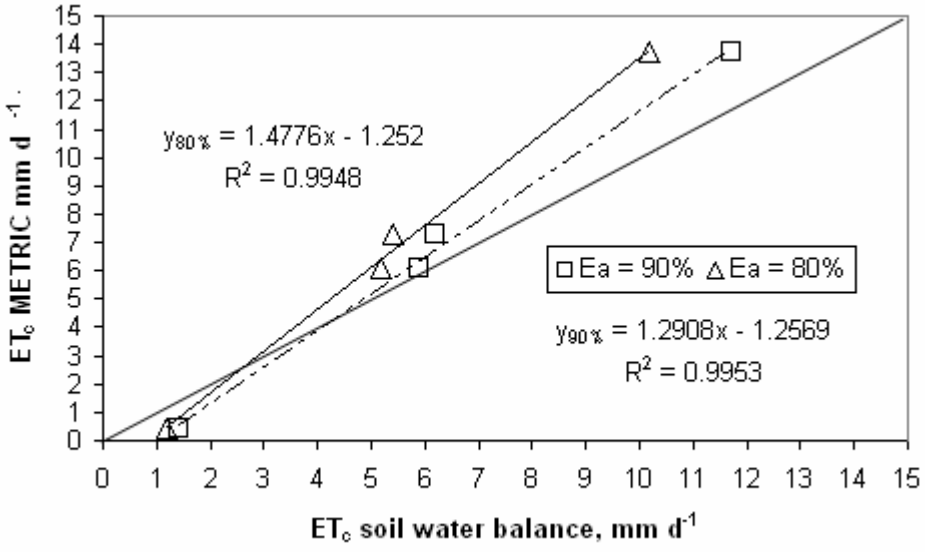

Figure 2. Comparison between METRIC™ and soil water balance based ET_c.

reported that the average ET for well irrigated corn on lysimeters, exceeded 10 mm d^{-1} (with a maximum ET slightly exceeding 14 mm d^{-1}) in mid and late June, when monthly average wind speeds were 4.0-5.5 m s^{-1}. They indicated that crop growth and yields were similar on both the lysimeters and in the fields and were representative of normal regional corn production. Irrigated corn ET values were closely followed by evaporation rates from open water bodies, mainly playas and ponds with 10.2±3.1 mm d^{-1}. Differences in the water and cropped surface (roughness length, heat storage and aerodynamic resistance) produce differences in water loss from an open water surface and the crop.

Overall, the daily ET results indicate that METRIC™ performs well for the advective conditions of the Texas High Plains with prediction errors of 4-20%. Some errors in the evaluation may have been introduced by the soil water content balance procedure and by the weather data. According to Wright and Jensen (1978), a common standard error for ET prediction equations based on weather data using Penman or Penman-Monteith type equations is as much as 10% of daily estimates.

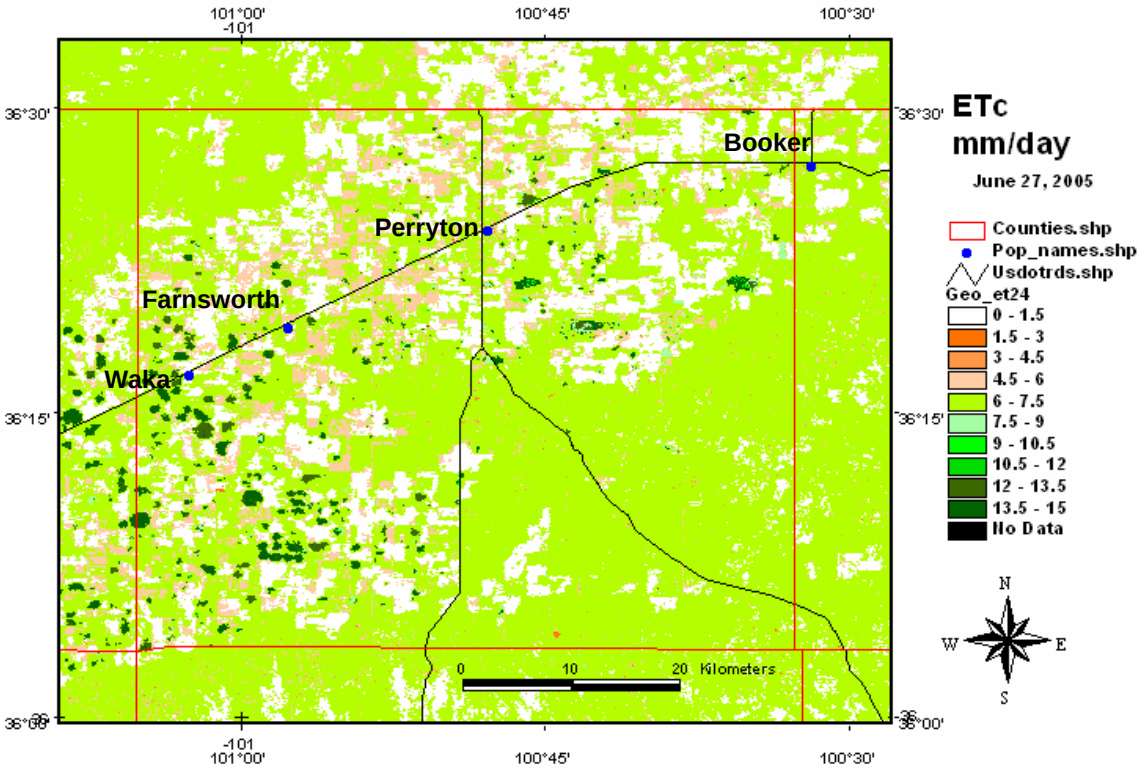

Figure 3. Spatially distributed daily ET for Ochiltree County on DOY 187

Conclusion

METRIC™ algorithm was applied on the Texas High Plains using a Landsat 5 TM image acquired on DOY 178. Estimated ET for well-irrigated crops and high biomass vegetation was estimated with errors below 15%. Errors were less than 9% for lower biomass-higher temperature surfaces. It is believed that the 5% increment over ET_r suggested in METRIC for the instantaneous ET estimation on the cold pixel, might have caused the overestimation of ET

on well watered crops with high ET with bio-physical characteristics that were different from the reference crop, i.e., with a crop coefficient greater than unity at the time of the remote sensing system imagery acquisition. However, ET estimates were compared with ET derived from soil water measurements using gypsum blocks that may have errors around 20% (Gardner, 1986)

Nevertheless, it appears that METRIC™ is a promising tool in estimating ET for well irrigated, medium to high biomass crops, natural vegetation and open water bodies as well as for low/drier biomass vegetation covers. Further, METRIC™ does not need ground information in terms of accurate surface and air temperature, planting date, land use and land cover. The only ground measured input needed is horizontal wind speed and dew point temperature.

Additional evaluation of METRIC™ is needed under a variety of crop/weather conditions to fully assess its capability to accurately estimate spatially distributed ET values, including evaluations with lysimetric data and/or a large number of satellite imagery scenes.

References

Allen, R.G., M. Tasumi, and A. Morse. 2005a. Satellite-based evapotranspiration by METRIC and Landsat for western states water management. US Bureau of Reclamation Evapotranspiration Workshop. Feb 8-10, 2005. Ft. Collins, CO.

Alllen, R.G., M. Tasumi, and R. Trezza. 2005b. METRIC: Mapping evapotranspiration at high resolution – Applications manual for landsat satellite imagery. University of Idaho. 130 p.

Amayreh, J.A. 1995. Lake evaporation: a model study. PhD Diss. Logan, UT: Utah State University, Biological and Irrigation Engineering Department.

Axtell, S. 2006. Ogallala initiative. Available at: http://ogallala.tamu.edu. Accessed on 20 November 2006.

Bastiaanssen, W.G.M. 2000. SEBAL-based sensible and latent heat fluxes in the irrigated Gediz Basin, Turkey. *J. Hydrol*., 229:87-1000.

Bastiaanssen, W.G.M., M. Menenti, R.A. Feddes, and A.A. Holtslang. 1998. A remote sensing surface energy balance algorithm for land (SEBAL): 1. Formulation. *J. Hydrol.* 212-213, 198-212.

Chander, G., and B. Markham. 2003. Revised Landsat-5 TM radiometric calibration procedures and postcalibration dynamic ranges. *IEEE Trans. on Geosc. and Remote Sens.* 41(11):2674-2677.

Chávez, J.L. 2005. Validating surface energy balance fluxes derived from airborne remote sensing. Ph.D. Diss. Logan, UT: Utah State University, Biological and Irrigation Engineering Department.

Chávez, J.L., C.M.U. Neale, L.E. Hipps, J.H. Prueger, and W.P. Kustas. 2005. Comparing aircraft-based remotely sensed energy balance fluxes with eddy covariance tower data using heat flux source area functions. *Journal of Hydrometeorology, AMS.* 6(6):923-940.

Chehbouni, A., Lo Seen, D., Njoku, E.G., Monteny, B.1996. Examination of the difference between radiative and aerodynamic surface temperatures over sparsely vegetated surfaces. *Remote Sens. Environ*. 58: 177–186.

Crago, R., M. Friedl, W. Kustas, and Y. Wang, 2003. Investigation of Aerodynamic and Radiometric land surface temperatures. NASA Scientific and Technical Aerospace Reports (STAR). Vol. 42(1).

Dennehy, K.F., 2000. High Plains regional ground-water study: U.S. Geological Survey Fact Sheet 091-00, 6 p.

Evans, R., Cassel, D.K., and R.E. Sneed. 1996. Measuring soil water for irrigation scheduling: Monitoring methods and devices, North Carolina Cooperative Extension Service. Available at: http://www.bae.ncsu.edu/programs/extension/evans/ag452-2.html. Accessed on 10 April 12, 2007

Foken, T. 2006. 50 Years of the Monin-Obukhov similarity theory. *Boundary-Layer Meteorol.* 119(3):431-447.

Frye, R.G, K.L. Brown, and C.A. McMahan. 2000. Vegetation/cover types of Texas. Bureau of Economic Geology. University of Texas at Austin. Available on line at: http://www.beg.utexas.edu/UTopia/images/pagesizemaps/vegetation.pdf. Accessed December 13 2006.

Gardner, W.H. 1986. 2nd Ed. Water Content, In Methods of soil analysis, ed. A. Klute. Am. Soc. Agron. Monograph, No. 9, Part 1. Madison, Wis.: Soil Sci. Soc. Amer.

Howell, T.A. 2000. Discussion of "Adjusting temperature parameters to reflect well-watered conditions." *J. of Irrig. and Drain. Engr. (ASCE)* 126(5):340-342.

Howell, T. A., Tolk, J. A., Schneider, A. D., and Evett, S. R. 1998. Evapotranspiration, yield, and water use efficiency of corn hybrids differing in maturity. *Agron. J.* 90(1): 3-9.

Howell, T.A., S.R. Evett, J.A. Tolk, A.D. Schneider, and J.L. Steiner. 1996. Evaporation of corn – Southern High Plains. pp. 158-166, in C.R. Camp, E.J. Sadler, and R.E. Yoder (eds.) *Evapotranspiration and Irrigation Scheduling, Proceedings of the International Conference,* Nov. 3-6, 1996, San Antonio, TX, American Society of Agricultural Engineers, St. Josepth, MI.

Kustas, W.P., J.L. Hatfield, and J.H. Prueger. 2005. The Soil Moisture-Atmosphere Coupling Experiment (SMACEX): Background, hydrometeorological conditions, and preliminary findings. *J. Hydrometeor.*, 6(6):791-804.

Linsley, R.K., J.B. Franzini, D.L. Freyberg, and G. Tchobanoglous. 1992. *Water resources engineering*. 4th ed., Irwin/McGraw-Hill. New York, NY.

NCSS Web Soil Survey. 2006. National Cooperative Soil Survey. Natural Resources Conservation Service. United States Department of Agriculture. Available on line at: http://websoilsurvey.nrcs.usda.gov/app/. Accessed on November 13 2006.

New, L. 2005. Agri-Partner irrigation result demonstrations, 2005. Texas Coop. Ext., Available at: http://amarillo.tamu.edu/programs/agripartners/irrigation2005.htm (accessed 7 Dec 2006).

New, L. and G. Fipps. 2000. *Center Pivot Irrigation*. Texas Agricultural Extension Service - The Texas A&M University System. Bulletin B-6096. p. 20.

Roberts, W.J., and J.B. Stall. 1967. *Lake evaporation in Illinois*. Illinois State Water Survey, Champaign, IL, 44p.

Rosenberg, N.J., B.L. Blad, and S.B. Verma. 1983. *Microclimate*, The Biological Environment, Second Edition. John Wiley & Sons, New York. 495 pp.

Tasumi, M. 2005. A review of evaporation research on Japanese lakes. In *Proc. 2005 EWRI Conf.*, Anchorage, Alaska, May 15-19.

Tasumi, M., R. Trezza, R.G. Allen, and J.L. Wright. 2005. Operational aspects of satellite-based energy balance models for irrigated crops in the semi-arid U.S. *J. Irrig. and Drainage Syst*. 19:355-376.

TXHPET. 2006. Texas High Plains Evapotranspiration Network. Available on line at: http://txhighplainset.tamu.edu/index.jsp. Accessed on September 4 2006.

TNPET. 2006. Texas North Plains ET Network. Available on line at: http://amarillo2.tamu.edu/nppet/petnet1.htm. Accessed on September 4 2006.

Tolk, J.A., S.R. Evett, and T.A. Howell. 2006. Advection influences on evapotranspiration of alfalfa in a semiarid climate. *Agron. J*. 98:1646-1654.

Trezza, R. 2002. Evapotranspiration using a satellite-based surface energy balance with standardized ground control. Ph.D. Diss. Logan, UT: Utah State University, Biological and Irrigation Engineering Department.

USDA-NASS. 2006. Texas crop acreage and production by County in PDF format. Available at: http://www.nass.usda.gov/Statistics_by_State/Texas/Publications/County_Estimates/ce_cp.htm. Accessed 10 October 2006.

Watson, I., and A.D. Burnett. 1995. *Hydrology: An Environmental Approach.* p. 425–427, Lewis Publishers, CRC Press LLC, Boca Raton, 702 p. ISBN 1-56670-087-6.

Wright, J.L., and M.E. Jensen. 1978. Development and evaluation of evapotranspiration models for irrigation scheduling. *Trans. ASAE* 21(1):88-96.

Yoder, R.E., D.L. Johnson, J.B. Wilkerson, and D.C. Yoder. 1998. Soil water sensor performance. *Appl. Eng. in Agric.* 14(2):121-133.